

## Electro chemical and photo catalytic studies of MnO<sub>2</sub> nanoparticle from waste dry cell batteries

M. Mylarappa<sup>1,2</sup>, V. Venkata Lakshmi<sup>\*1</sup>, K. R. Vishnu Mahesh<sup>\*\*3</sup>, H. P. Nagaswarupa<sup>4</sup>,  
S. C. Prashantha<sup>4</sup>, D. M. K. Siddeswara<sup>4</sup> and N. Raghavendra<sup>5</sup>

<sup>1</sup>Research Centre, Department of Chemistry, AMC Engineering College, Bengaluru-560083, Karnataka, India

<sup>2</sup>Department of Studies and Research in Chemistry, Tumkur University, Tumkur-572103, Karnataka, India

<sup>3</sup>Department of Chemistry, Dayananda Sagar College of Engineering, Bengaluru-560083, Karnataka, India

<sup>4</sup>Research Centre, Department of Science, East West Institute of Technology, Bengaluru-560091, Karnataka, India

<sup>5</sup>CMRTU, RV College of Engineering, Bengaluru-560059, Karnataka, India

\*laxmimurthy@rediffmail.com, \*\*vishnumaheshkr@gmail.com

PACS 82.47.-a

DOI 10.17586/2220-8054-2016-7-4-657-661

The objective of the existing research was essentially focused on recovery of MnO<sub>2</sub> nanoparticles from consumed dry cells by employing adapted hydrometallurgical process. Experimental tests for the recovery of MnO<sub>2</sub> present in the dry cell batteries have been carried out by an acidic reductive leachant, namely oxalic acid. The elemental compositions of the recovered metals from dry cells were confirmed by Energy Dispersive X-ray analysis (EDAX). Surface morphology of the recovered metals was examined using Scanning Electron Microscopy (SEM). Phase composition of the recovered metals from dry cell batteries were confirmed from X-ray Diffract meter (XRD). Cyclic Voltammetry (CV) studies were carried out to clarify the reversibility of the reactions. The obtained MnO<sub>2</sub> catalyst was applied for the degradation of different non-volatile dye compounds such as Indigo carmine (IC) and Rhodamine B (RB). The performance of MnO<sub>2</sub> shows fast degradation of dyes of high concentration.

**Keywords:** Dry cell batteries, recovery, Zn, Mn, electrochemical, catalytic activity.

*Received: 5 February 2016*

### 1. Introduction

Dry cell batteries are used in radios, recorders, toys, remote controls, watches, calculators, cameras, and in many other objects. The waste batteries present serious problems due to their toxicity, abundance and longevity in the environment [1]. The hydrometallurgical methods are the most popular process in all over the world because of its environmental suitability and economical costs for treating even low zinc and manganese containing materials on small scale with high purity and low energy requirements [2, 3]. Hence, the treatment of these wastes for the recovery of manganese is vigorous for discarded material to raw material recycling. Two different acid-reductive leaching agents have been investigated; sulfuric acid - oxalic acid and sulfuric acid- hydrogen peroxide. MnO<sub>2</sub> is economically and commercially-important with applications in different fields, such as battery industry, catalysis, water treatment plants, steel industry and chemicals. In this study, we show how to recover manganese as MnO<sub>2</sub> from consumed dry cell using a hydrometallurgical process, without altering the concentration of zinc in solutions that can be recovered by precipitation or electro winning [4]. The aim of this work is to study the applicability of electrochemical and photocatalytic enactment of MnO<sub>2</sub> using a hydrometallurgical process and the catalytic action of MnO<sub>2</sub> is due to its high efficiency in the reduction/oxidation cycles [1]. The effects of the recovered conditions and crystallinity of MnO<sub>2</sub> on the catalytic performance in degradation of high concentration dyes (methylene blue indigo carmine and Rhodamine B) were intensively evaluated [5]. Nanostructured materials have received enormous interest in recent years because of their unusual properties when compared with bulk materials. Nanoscale one-dimensional (1D) structures such as nanotubes, nanowires and nanorods have attracted much interest because of their unique electronic, optical and mechanical properties due to the low dimensionality and the quantum confinement effect. For example, the electrons interact differently in one dimensional (1D) and three-dimensional structures (3D). The 1D system is the smallest dimensional structure that can be used for efficient transport of electrons and optical excitations, and is thus expected to be critical to the function and integration of nanoscale devices. 1D nanostructure provides a good system for investigating the electrical and thermal transport properties in size and shape reduction [6–8]. The aim of this work is to study the applicability of electrochemical and photocatalytic enactment of MnO<sub>2</sub> using a hydrometallurgical process and the catalytic action of MnO<sub>2</sub> is due to their high efficiency in the reaction/oxidation cycles [1]. The effects of the recovered conditions and crystallinity of MnO<sub>2</sub> on the catalytic performance in degradation of high concentration dyes (methylene blue indigo carmine and Rhodamine B) were thoroughly evaluated [5].

## 2. Experimental

The waste dry cell batteries in an amount of 100 g were collected from different manufacturers. A series of mechanical processing is conducted in the following sequence to yield enriched Zn and Mn particles. The waste dry cell batteries were fed to a hammer mill for dismantling. Magnetic separator removed the magnetic fractions and the non-magnetic fraction was screened in a 2 mm sieve. A second magnetic separation was carried out to remove the ferrous materials which remain in the sample. The sieved powder was later washed with deionized water and finally dried at 100 °C for 24 hrs. The washed powder (20 g) was subsequently dissolved in 100 mL, 3 M H<sub>2</sub>SO<sub>4</sub> followed by addition of 5.94 g Oxalic acid dehydrated as leaching agent. The leaching was continued for 5 hrs at 90 °C with continuous stirring. Recovery of MnO<sub>2</sub> particle from the leaching solution is possible at room temperature without special purification of the solution, and preserving a high efficiency. After the complete reductive acid leaching process, the required quantity of leached solution in a 500 ml beaker and a solution of 4 M NaOH was added slowly to the beaker with constant magnetic stirring. At the end of the precipitation, the solution in the beaker was filtered and the solid residue remaining in the filter paper was dried in an oven at 100 °C for 24 hours. MnO<sub>2</sub> was formed as dark precipitate at the bottom of the cell. The recovered sample was investigated by means of the EDX, SEM and XRD to analyze elemental composition, morphology and phase composition of the powder.

## 3. Result and discussion

Energy Dispersive X-ray analysis (EDX) was carried out to obtain the elemental composition of the metals in powder sample. The accurate size and morphology of the MnO<sub>2</sub> studied from the Scanning Electron Microscopy (SEM) and X-ray diffraction spectroscopy (XRD). Fig. 1(a) shows that manganese and oxygen contents were detected in that point, indicating the presence of high manganese hydroxide content [9]. The leaching residue showed almost similar particle size compared to that before leaching. Particles are well distributed throughout with little agglomeration; particle sizes ranged from 5 to 30 μm. In Fig. 1(b), the average particle size of MnO<sub>2</sub> is found to be 9 nm, indicating good crystallinity.

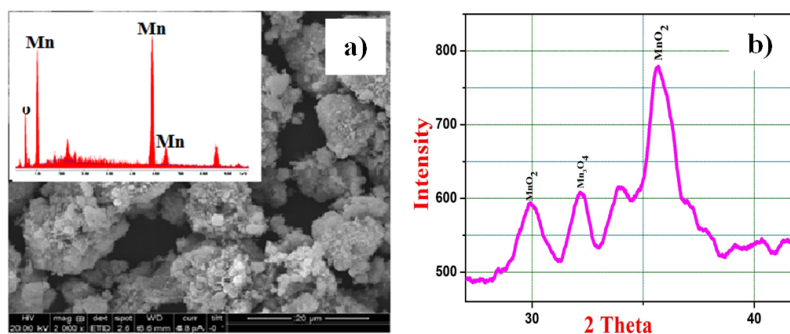


FIG. 1. EDAX/SEM and XRD spectra of MnO<sub>2</sub> from dry cells

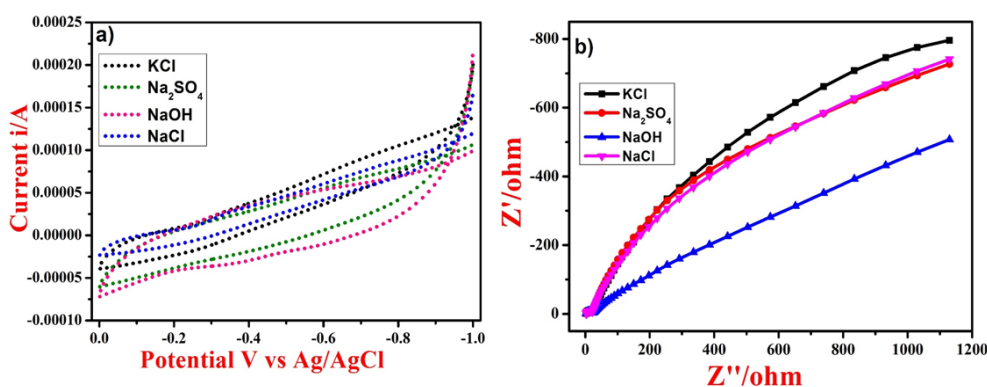
## 4. Cyclic voltammetry studies

The MnO<sub>2</sub> electrode was prepared as a commixture with 10 wt.% of MnO<sub>2</sub> powder as active material with 90 wt.% of graphite. The constituents were mixed along with 3 drops of silicone oil to obtain uniform composition. Electrochemical activity of MnO<sub>2</sub> is often assessed by CV and electrochemical impedance spectra (EIS). An electrochemical measurement utilizes a three-electrode system having working electrode, Ag/AgCl reference electrode and a platinum wire as counter electrode. Cyclic voltammetry (CV) and EIS were performed in potential between +0 to -1 V using 0.5 M KCl, NaOH, Na<sub>2</sub>SO<sub>4</sub> and NaCl electrolytes at a constant scan rate [6, 10]. To evaluate the electrochemical reversibility ( $E_R$ ) of the sample, the potential window of CV was changed from +0 to -1 V and sweep rate 10 mV as shown in Fig. 2(a). A smaller the value of  $E_0 - E_R$  shows the reversibility of the electrode reaction is greater. In Figs. 2(a) and 2(b), it is clearly shown that the smaller the value of  $E_0 - E_R$ , the greater the reversibility of the electrode reaction is. Samples having lower solution resistance values ( $R_s$ ) are going higher conductivity values. In Figs. 2(a) and 2(b), it is readily seen that the MnO<sub>2</sub> sample using 0.5 M NaOH has lower  $E_R$  compare to different electrolytes, indicating the higher conductivity. The comparative cyclovoltammetric results of electrode in several electrolytes at a scan rate of 10 mV/s are tabulated in Table 1. Fig. 3(a) to (d) show the different scan rates with different electrolytes. The effect of scan rate is presented in Fig. 3. As the

TABLE 1. Electrochemical reversibility

Electrolytes	E <sub>0</sub> (mV)	E <sub>R</sub> (mV)	E <sub>0</sub> – E <sub>R</sub>	R <sub>ct</sub> (ohm)	C(F) × 10 <sup>-5</sup>
0.5 M KCl	0.3951	0.3373	0.0578	15.75	0.0282
0.5 M NaOH	0.3040	0.3261	0.0221	15.15	0.01594
0.5 M Na <sub>2</sub> SO <sub>4</sub>	0.4443	0.3939	0.0504	22.28	0.01285
0.5 M NaCl	0.8268	0.3569	0.4699	19.26	0.01414

scan rate increases, the CV profile deviates from the ideal capacitive behavior. This is mainly because the redox reactions depend on the insertion-deinsertion of the alkali ion or protons from the electrolyte. At slower scan rates, the diffusion of ions from the electrolyte can gain access to almost all available pores on the electrode surface, leading to a complete insertion reaction, indicating excellent capacitive behavior and a low contact resistance. However, the curve shape is gradually distorted from rectangular to quasi-rectangular with an increase of the scan rate from 10 mV/s to 50 mV/s. The experimental information shows the redox reactions for all electrolytes, as indicated by the moderately large  $E_0 - E_R$  and  $R_{ct}$ . However, the  $E_0 - E_R$  of electrode in 0.5 M NaOH was merely 0.0221 mV and 15.15 Ω, as shown in Fig. 4(a) to (d), which is smaller than that of the different electrolytes as seen the Table 1. This indicates that the capacitive behavior of the given electrode in 0.5 M NaOH is better than the other electrolytes.

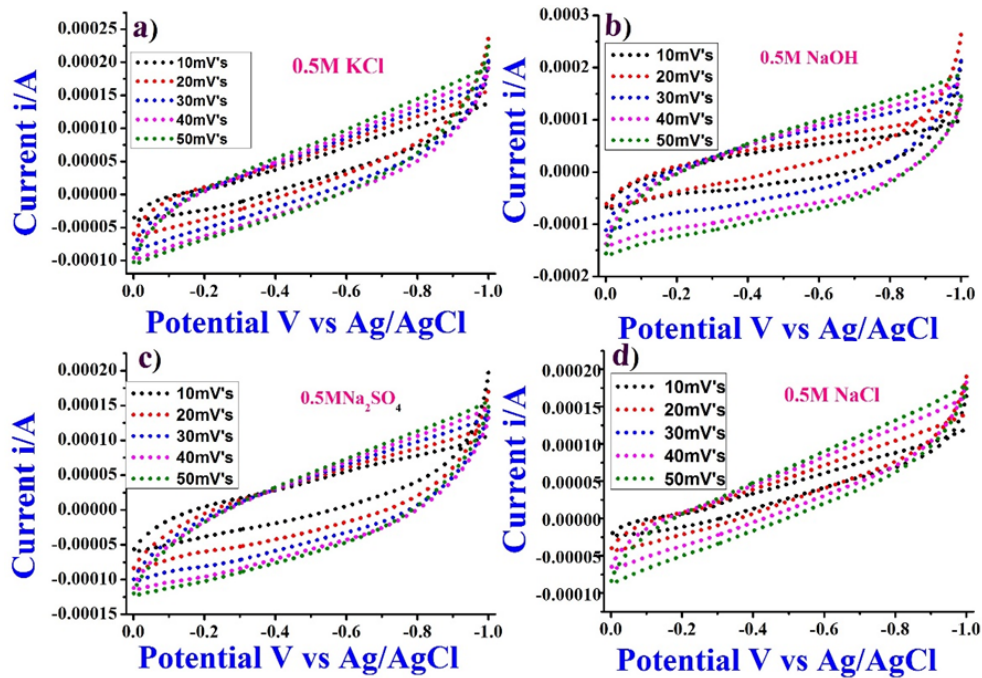
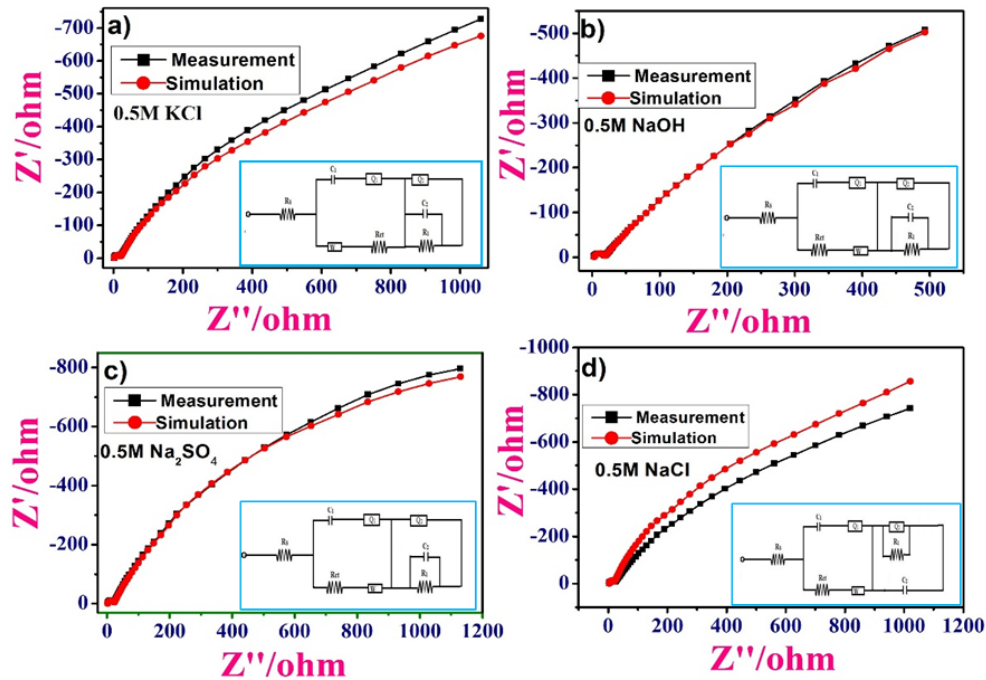
FIG. 2. a) Cyclic voltammograms of MnO<sub>2</sub> different electrolytes; b) Impedance spectra of MnO<sub>2</sub> electrode

## 5. Photocatalytic Activity of MnO<sub>2</sub>

The photocatalytic enactment of the as-prepared sample was assessed through the photocatalytic degradation of Rhodamine-B (RB) and Indigo carmine (IC) under visible light irradiation. In these experiments, 60 mg of MnO<sub>2</sub> was dispersed in 250 ml IC (20 ppm) and similarly Rhodamine-B aqueous solutions respectively. The mixed suspensions were first magnetically stirred in the dark for 30 min to reach the adsorption-desorption equilibrium. Under stirring at ambient conditions, the mixed suspensions were exposed to visible light irradiation produced by a 400 W metal Philips lamp (wavelength: 254 nm). At certain time intervals, 5 ml aliquots of the mixed suspensions were extracted. The filtrates were analyzed by recording UV-vis spectra of RB and IC using a Spectratreats 3.11.01 Release 2A UV-vis spectrophotometer. The UV-vis absorption of MnO<sub>2</sub> show an intense absorption band in the range 200 to 220 nm. In Fig. 5 shows the UV-vis absorption spectra of RB and IC as a function of the catalytic reaction time [11]. Both RB and IC solutions turns colorless after 30 min, which indicates complete degradation of the dye molecules by MnO<sub>2</sub>. After 30 min of reaction, the MnO<sub>2</sub> showed a higher efficiency in degradation of IC compared to RB. During the process of IC and RB degradation, the MnO<sub>2</sub> is reduced to Mn<sup>2+</sup>, and leaches into the water and 74 % degradation is achieved under optimal conditions. It was determined that using the as-recovered MnO<sub>2</sub> Nano particle from waste dry cells, the dye solutions with concentration 60 mg/L can be degraded up to 74 % and mineralized up to 24 % in 45 minutes.

## 6. Conclusion

In this study, an aqueous technique was utilized to recover MnO<sub>2</sub> nanoparticles from waste dry cells by hydrometallurgy. Highly porous nano-MnO<sub>2</sub> is effectively recovered. Electrochemical estimations meant that the

FIG. 3. Different scan rate of  $\text{MnO}_2$  in different electrolytesFIG. 4. Nyquist plots and equivalent circuit for  $\text{MnO}_2$  electrode in different electrolytes

$\text{MnO}_2$  obtained displayed high electrochemical activity when the precipitates are kept at  $100^\circ\text{C}$  for 24 hrs. The electric limit of this example demonstrated to be superior in correlation with the business tests. This showed that the  $\text{MnO}_2$  had the best electrochemical execution at a high sweep rate of  $10\text{ mV/s}$ . The recovered specimen displayed low charge exchange resistance ( $R_{ct}$ ) and high capacitive authorization. The morphology and crystallinity of  $\text{MnO}_2$  improve in catalytic enactment in degradation of RB and IC. Using the as-obtained  $\text{MnO}_2$ , the IC solution with concentration  $60\text{ mg/L}$  was shown to be degraded up to  $74\%$  and mineralized up to  $24\%$  and RB up to  $72\%$  in 45 minutes.

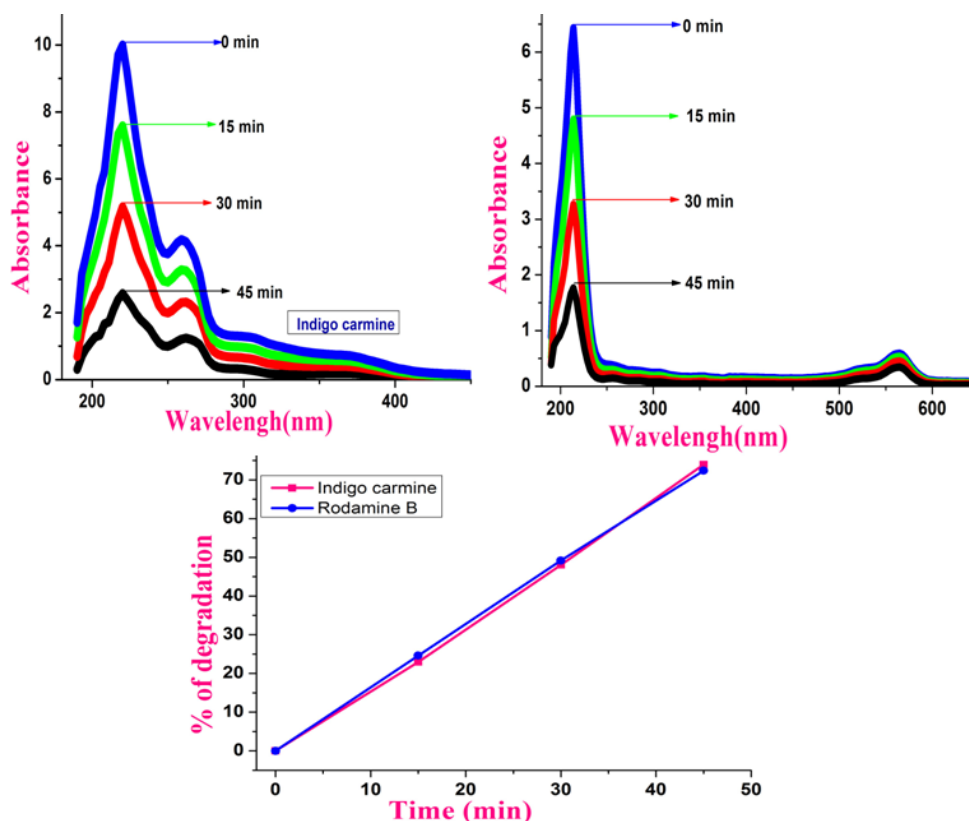


FIG. 5. UV-vis absorption spectra of RB and IC as role of time catalyzed by MnO<sub>2</sub>

## References

- [1] Gallegos M.V., Falco L.R., et al. Recovery of manganese oxides from spent alkaline and zinc-carbon batteries. An application as catalysts for VOCs elimination. *Waste Management*, 2013, **33**, P. 1483–1490.
- [2] Sobianowska-Turek A., Szczepaniak W., Zab-locka-Malicka M. Electrochemical evolution of reducers – Recovery of Mn from Zinc-Mn and Zinc-C battery waste. *Journal of Power Sources*, 2014, **270**, P. 668–674.
- [3] Baba A.A., Adekola A.F., Bale R.B. Development of a combined pyro-and hydro-metallurgical route to treat spent Zinc-carbon batteries. *Journal of power sources*, 2009, **171**, P. 838–844.
- [4] Macolino P., Manciulea A.L., et al. Manganese recovering from alkaline spent batteries by ammonium peroxodisulfate. *Acta Metallurgica Slovaca*, 2013, **19** (3), P. 212–222.
- [5] Andrade Tacca C.A., Duart M.M.E. Acid leaching and electrochemical recovery of manganese from spent alkaline batteries. 2nd Mercosur Congress on Chemical Engineering and 4th Mercosur Congress on Process Systems Engineering.
- [6] SiXu Deng, Dan Sun, et al. Synthesis and electrochemical properties of MnO<sub>2</sub> nanorods/graphene composites for supercapacitor applications. *Electrochimica Acta*, 2013, **111**, P. 707–712.
- [7] Devreese J.T., Evrard R.P., Van Doren V.E. *Highly Conducting One-Dimensional Solids*. Plenum, New York, 1979.
- [8] Pandey B.K., Shahi A.K., Gopal R. Synthesis, optical properties and growth mechanism of MnO nano structures. *Applied Surface Science*, 2013, **283**, P. 430–437.
- [9] Kursunoglu S., Kavva M. Dissolution and precipitation of Zinc and Manganese obtained from spent Zinc-carbon and alkaline battery powder. *Physicochem. Probl. Miner Process*, 2014, **50**, P. 39–53.
- [10] Buzatu M., Aceanu S.S., et al. Recovery of zinc and manganese from spent batteries by reductive leaching in acidic media. *Journal of power sources*, 2014, **247**, P. 612–617.
- [11] Chanhlin Yu, Gao Li, et al. Fabrication, characterization of  $\beta$ -MnO<sub>2</sub> micro rod catalysts and their performance in rapid degradation of dyes of high concentration. *Catalysis Today*, 2014, **224**, P. 154–162.